Modeling Research Reactor Fuel Plate Hotspots with COMSOL's Thin Layer and Thermal Contact Features

Michael J. Richards[*1], Arthur E. Ruggles[1], James D. Freels[2]
[1]The University of Tennessee, [2]Oak Ridge National Laboratory
*Corresponding author: 5029 Jade Pasture Ln, Knoxville, TN 37918, richardsfamily.mike@gmail.com

Abstract: One challenge with converting nuclear research reactors to low enrichment fuels is the thermal-fluid performance of those fuels. Local areas of high temperature, known as hotspots, limit reactor performance and thus require accurate modeling. A simplified fuel plate model is developed to compare traditional FEA techniques with COMSOL's thin layer (TL) and thermal contact (TC) features for modeling regions of low thermal conductivity and high energy generation that produce hotspots. Temperatures, conductive heat fluxes, and energy balances are reported. TL and TC offer similar performance with < 0.3% error in energy balance for all cases. Both experience oscillations in boundary, normal heat flux at discontinuities in conductivity that decrease with grid refinement and increased element order. TC offers options that make it more appropriate for hotspot models.

Keywords: hotspot, thermal contact, thin layer

1. Introduction

Nuclear research reactors offer unique capabilities that provide opportunities for material irradiation and neutron scattering not available in power reactors. The use of high enriched uranium (HEU) in some research reactors creates a nuclear material proliferation vulnerability. To help prevent proliferation of nuclear weapons while allowing the continued use of these reactors, efforts are underway to convert from HEU to low enriched uranium (LEU) fuel. Among the challenges with this conversion is the thermal-fluid performance of the fuel.

A typical fuel plate consists of fuel sandwiched between aluminum cladding. During the manufacturing process two defects of interest may occur. First, the fuel may not be distributed evenly and local areas of higher enrichment, known as fuel segregations, may result. These generate more energy than the surrounding fuel. Second, the fuel plate may contain non-bonds, regions where the cladding does not bond to the fuel. These reduce the thermal conductivity across the fuel-cladding interface which creates a hotspot on the opposite side of the plate. The worst case scenario is when these two defects are coincident.

Hotspots caused by these defects limit plate-fueled research reactor performance. Accurate modeling of hotspots is required for qualification of new LEU fuels and also improves the safety analysis and operations for current HEU fuels. A portion of this effort to improve hotspot models is to accurately model non-bonds, which is the focus of this paper.

2. Numerical Model

For this study, a simplified 2D model of a fuel plate was developed, shown in Figure 1. The cladding is 38.1 mm [1.5 in] long and 1.27 mm [0.05 in] thick. The fuel is centered within the cladding and is 25.4 mm [1 in] long and 0.76 mm [0.03 in] thick.

A number of simplifying assumptions were made in the development of the model. The first is that the defect-free portion of the fuel experiences uniform energy generation. In reality, the configuration of the fuel plate within the reactor will cause variations in energy generation across the fueled region. A second assumption is that a constant convective heat transfer coefficient exists with a constant coolant temperature adjacent to the fuel plate. In reality, the fuel plate is submerged in a distributed turbulent flow of coolant that warms as it flows across the plate.

The built-in material properties for aluminum were used for both cladding and fuel. Heat generation rates and the convective heat transfer rate were set to 1.63e10 W/m^3 and 85.2 $W/(m^2 K)$ respectively. The fluid temperature was set to 322 K [120°F] for the convective boundary condition. The left and right edges of the model were insulated.

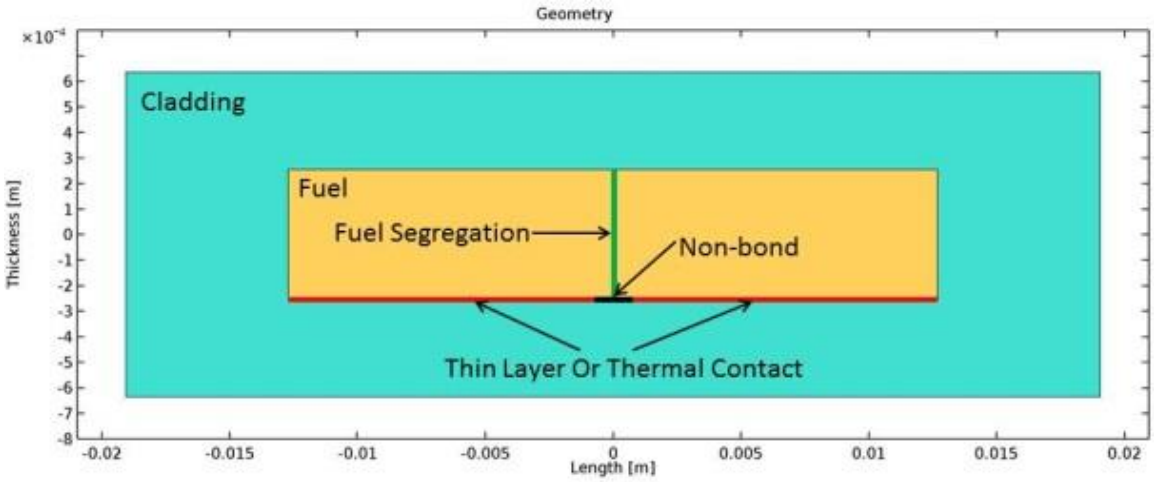

Figure 1 Simplified fuel plate model including a fuel segregation (green), altered boundary (red), and a non-bond/adiabatic disc (black) [Note that the vertical scale is significantly enlarged].

The meshes were generated using the semiconductor settings with free quadrilaterals, and the built-in mesh-density sizes.

3. Use of COMSOL Multiphysics® Software

Nuclear fuel plates present a conjugate heat transfer challenge. Energy produced within the fuel plate is conducted through the fuel plate and into the flowing coolant. The primary equations describing these processes are an energy balance on both the fuel plate and the coolant, and the continuity equation and Navier-Stokes equations on the coolant. The simplifying assumptions of a constant convective heat transfer coefficient and constant bulk fluid temperature, mentioned above, reduce the equations describing the fluid to a boundary condition in the fuel plate energy balance.

The focus of this effort was on modeling non-bonds. Historically, the non-bond has been modeled as an adiabatic disc between the fuel and the cladding [1-4]. This results in a conservative prediction of the peak cladding surface temperature. By more accurately modeling the non-bond, some of this conservativeness may be reduced while still maintaining appropriate safety margins.

While the non-bond can be, and has been, modeled using traditional FEA techniques, this requires the generation of a very fine mesh in the vicinity of the non-bond. COMSOL Multiphysics offers two features, thin layer and thermal contact, that may be used to model a non-bond with reduced mesh requirements.

3.1 Thin Layer

For the thin layer and thermal contact models, the bottom of the fuel portion, the red line in Figure 1, was used as the altered boundary. For these features to be of value, the temperature fields and heat fluxes should approach what would be expected without a modified boundary. To make this happen, the heat flux through the altered boundary had to be as similar to the unaltered boundary as possible.

The thin layer is mathematically modeled as

$$-\boldsymbol{n}_d \cdot \boldsymbol{q}_d = -k_s \frac{T_u - T_d}{d_s}$$

where the d and u subscripts indicate the "up" and "down" side of the boundary, k_s is the thermal conductivity of the layer, and d_s is the thickness of the boundary. The up and down side of the boundary represent the same location and operate at co-incident nodes between two domains. When the boundary is between two materials with different thermal conductivities the geometric mean of the two conductivities is used. Within COMSOL Multiphysics the options available are to use the material properties of the two surfaces to determine the conductivity or to provide a user-defined thermal conductivity. For this model, the built-in material properties were used, and a thin layer thickness of 1 µm [39 µin] was used.

3.2 Thermal Contact

COMSOL Multiphysics offers two models for thermal contact conductance: CMY for plastic contact and Mikic for elastic contact. This study used the Mikic model because the non-bond contact is elastic. The model is represented mathematically by

$$-\boldsymbol{n}_d \cdot \boldsymbol{q}_d = -h_c(T_u - T_d) + rQ_b \quad \textbf{(1)}$$

with

$$h_c = 1.54 k_c \frac{m_{asp}}{\sigma_{asp}} \left(\frac{\sqrt{2}p}{m_{asp} E'} \right)^{0.94}.$$

where m_{asp} is the average slope of the surface topology, σ_{asp} is the average asperity height, or surface roughness, E' is the reduced modulus of the two materials, k_c is the geometric mean of the thermal conductivity of the two materials, and p is the contact pressure between the two surfaces. Q_b is for heat generation within the boundary. As explained above, in order to reduce the impact of the altered boundary on the temperature field, the heat transfer through this thermal contact boundary should equal that through an unaltered boundary. The following steps were taken to achieve this result. By rearranging the conductance relationship, h_c becomes

$$h_c = \left[1.54\, m_{asp}^{0.06} \left(\frac{\sqrt{2}p}{E'} \right)^{0.94} \right] \frac{k_c}{\sigma_{asp}}.$$

By substituting this into (1), and by assuming heat transfer can only occur normal to the contact and that there is no heat generation within the boundary, this can be rewritten as

$$-q_{tc} = \left[1.54\, m_{asp}^{0.06} \left(\frac{\sqrt{2}p}{E'} \right)^{0.94} \right] \frac{k_c}{\sigma_{asp}} (T_u - T_d).$$

By letting

$$C_{tc} = 1.54\, m_{asp}^{0.06} \left(\frac{\sqrt{2}p}{E'} \right)^{0.94}$$

This becomes

$$-q_{tc} = C_{tc}\, k_c \frac{T_u - T_d}{\sigma_{asp}}.$$

Recognizing that σ_{asp}, the mean asperity height of the surfaces in contact, is the un-modeled length separating the up and down temperature, it can be seen that this is essentially Fourier's law with an added coefficient, C_{tc}. This coefficient can be thought of as the modification to heat transfer due to the constrictions imposed by the contacting surfaces. In order to make this heat transfer equal to what would take place if there were complete thermal contact, this coefficient must equal 1.

Uncertainty in the values for m_{asp} and σ_{asp} typical for a non-bond, suggested they be examined in a later sensitivity analysis. For this study, values of 1 µm [39 µin] for the asperity height, a slope of 0.2 and the corresponding $\frac{p}{E'}$ of 0.4950 (to bring C_{tc} to 1) were used.

4. Method

The purpose in examining the thin layer and thermal contact features was to evaluate their ability to simulate a non-bond between the fuel and cladding. To this end, an adiabatic disk was introduced as a model for a non-bond in the thin layer boundary. This mimics how non-bonds have been modeled in the past. The adiabatic disc was produced by using a function to provide the user-defined thermal conductivity within the thin layer. The center 1.59 mm [0.0625 in], a length corresponding to the maximum acceptance criteria for non-bond inspections, of the function was set to 0 W/(m K) while the remainder of the length was set to the thermal conductivity of the material. A 0.254 mm [0.01 inch] transition, an arbitrarily chosen length, was included to soften the otherwise discontinuous thermal conductivities. The transition maintained a continuous second derivative.

The non-bond was similarly simulated in the thermal contact boundary: a function was developed where 1.59 mm [0.0625 in] at the center of the boundary used the realistic values of 3.1 MPa [450 psi] for the contact pressure and 70 GPa for the reduced modulus, while the remainder of the boundary used the same 0.4950 ratio for $\frac{p}{E'}$ identified above. Again, a 0.254 mm [0.01 in] transition region was used between these two values. This function of pressure over elastic modulus was then supplied in the "pressure" field and 1.0 was supplied in the "elastic modulus" field of the thermal contact menu.

To simulate the non-bond directly in the base model, a geometric entity with the same length and a 1 µm thickness was inserted at the center of the plate immediately below the fuel. The non-bond was assigned aluminum properties, as well, though the thermal conductivity set to 0.001 W/(m K) to model extremely poor conductivity.

A fuel segregation, which introduced higher heat flux as well as a region with significantly lower thermal conductivity, was modeled with the addition of a geometric feature. The built in aluminum properties were again used, except that the thermal conductivity was lowered to 25% of the value for aluminum. The energy generation rate for the fuel segregations was set to 10.3 times the fuel generation rate. At 0.417 mm [.0164 in] long and the thickness of the fuel, the fuel segregation was located at the center of the model and is shown in green in Figure 1.

A number of cases were run (1) to observe how the inclusion of TL and TC boundaries without non-bonds or fuel segregations change the results of the base model, (2) to compare the results of models with non-bonds created with TL, TC and by conventional FEA methods, and (3) to observe the effects of the inclusion of fuel segregations both independent of and coincident with non-bonds.

5. Results

The analysis examined the temperature distribution, the energy balances, and behavior of the heat fluxes within each model. The visual appearance of the results was very similar, and in some cases indistinguishable between the three modeling options (base, thin layer, and thermal contact).

5.1 Models without Fuel Defects

All three models without the presence of fuel defects produced visually indistinguishable temperature fields, Figure 2. By subtracting the results of the base model from the results of the models with the thin layer or thermal contact boundaries, a maximum difference of 1e-2 K was observed.

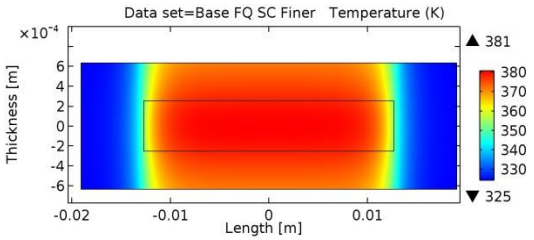

Figure 2 Temperature field of base case without fuel segregations or non-bonds.

Energy balance errors were evaluated by subtracting the energy leaving through the boundaries of each domain from the energy generated within those boundaries, and dividing that by the energy generated.

The base model showed no error in energy balance. Both TC and TL showed very similar errors to one another (identical to >4 digits of accuracy), shown in Table 1. Within this table, Fine, Finer, and Extra Fine refer to the built-in sizes for mesh generation.

Table 1: Errors in energy balance for both TL and TC at different grid refinements for the base case without fuel-defects or non-bonds.

	Grid		
Domain	Fine	Finer	Extra Fine
Fuel	0.0759%	0.0217%	0.0107%
Whole Model	0.0000%	0.0000%	0.0000%

The normal heat flux along the modified (TL or TC) boundary was very similar to that seen from the base model, except near the edges, where the modified boundaries oscillated and terminated at 0 while the base remained smooth and did not drop to 0, Figure 3.

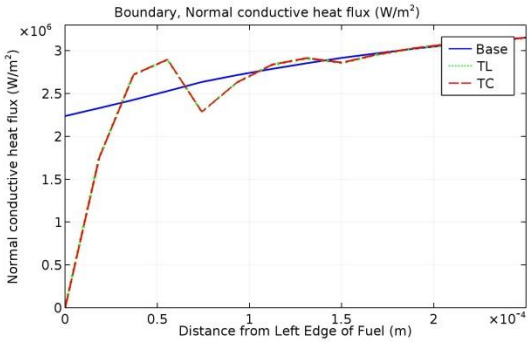

Figure 3 Comparison of the boundary, normal heat flux along the modified boundary for the base case without fuel segregations or non-bonds.

5.2 Models with Simulated Non-bonds

Introduction of a non-bond produces a localized hotspot at the surface of the fuel plate opposite from the non-bond. The intensity of the hotspot depends on the conductivity through the non-bond. Figure 4 shows the temperature increase caused by an adiabatic non-bond. The figure was generated by subtracting the results of the defect-

free base model from the TL with an adiabatic disc model.

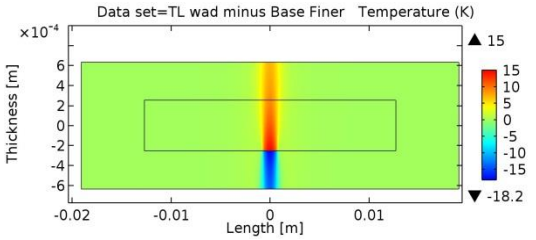

Figure 4 Temperature increase caused by an adiabatic non-bond.

Table 2 shows the maximum temperatures predicted and the maximum increase in temperature over the defect-free base.

Table 2: Maximum temperature (K) predicted and increase in temperature over the defect-free base caused by an adiabatic (wad) or a conductive (wnb) non-bond.

	Base wad	TL wad	TC wnb
max	393	393	390
increase	14.4	15	11.6

Introduction of a non-bond, either adiabatic or conductive, causes only minor changes (<0.0002%) in the energy balance errors for the TL or TC, however the energy balance for the base with a geometric, adiabatic non-bond experiences an error in energy balance of 0.062% across the fuel domain, which does not change when going from the Finer to Extra Fine grid.

In addition to the edge of the altered boundary, introduction of a non-bond also introduces oscillations in the flux along the boundary near the non-bond, Figure 5

.

5.3 Models with Simulated Fuel Segregations

The addition of a fuel segregation increases the local temperature field, Figure 6, as well as the maximum temperature experienced to 490 K. TL and TC show a maximum difference of 0.281 K from the base model with a fuel segregation.

Inclusion of fuel segregations also results in larger errors in energy balance in TL and TC, but no errors in the base model with a fuel segregation, Table 3. Oscillations in boundary and domain conductive heat flux along the altered boundary, Figure 7, are not as severe as with a non-bond. This plot shows just to the left of center of the fuel plate where the discontinuity in conductive heat flux, due to the discontinuity in thermal conductivity between the fuel segregation and the fuel, is captured.

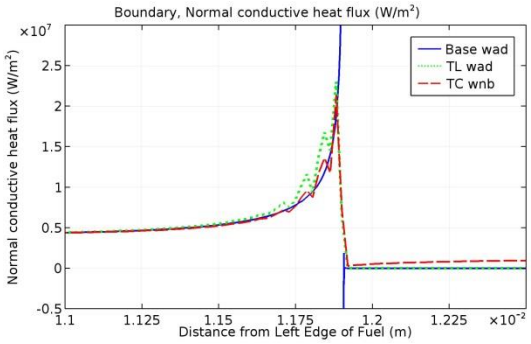

Figure 5 Oscillations experienced by TL and TC with the introduction of a simulated non-bond along the modified boundary.

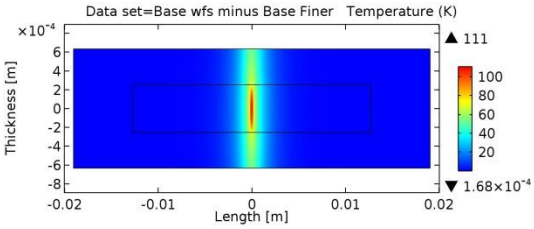

Figure 6 Temperature increase caused by a fuel segregation.

5.4 Models with Simulated Coincident Non-bonds and Fuel Segregations

A coincident non-bond and fuel segregation represents the worst case scenario for hotspots and leads to higher temperatures. Table 4 shows the maximum temperatures and the maximum increase in temperature relative to the base model with a fuel segregation (wfs) as well as the increase over the base model with no fuel defects.

A coincident non-bond and fuel segregation introduces energy balance errors in the base model as well as differences between TC and TL in these errors as shown in Table 5.

The oscillations in boundary conductive heat flux were more severe with the combination of non-bond and fuel segregation than with a non-bond alone as shown by Figure 8.

Table 3: Errors in energy balance for both TL and TC at different grid refinements for a defect case of fuel segregation only.

	Grid	
Domain	Finer	Extra Fine
Fuel Segregation (FS)	-0.229%	-0.122%
Fuel + FS	0.019%	0.010%
Whole Model	0.000%	0.000%

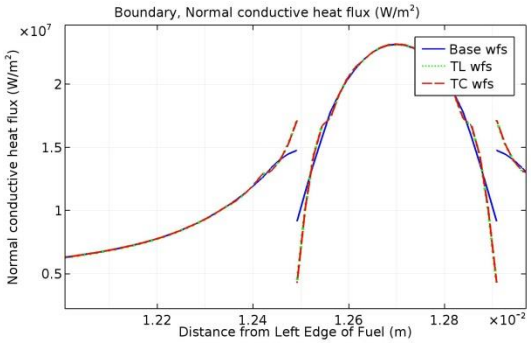

Figure 7 Oscillations experienced by TL and TC with the introduction of a simulated fuel segregation along the modified boundary.

Table 4: Temperature results with the inclusion of coincident fuel segregations and adiabatic (Base and TL) and conducive (TC) non-bonds.

	Base	TL	TC
maximum	546	548	537
minus Base wfs	97.4	99.4	87
minus Base	167	169	157

5.5 Flux Response to Grid Refinement and Element Order

All of the previous flux figures have been produced with results from the Finer grid size. Figure 9 shows how the oscillations in the flux near the edge of the non-bond change with grid refinement for a TL model with an adiabatic non-bond but no fuel segregation. AMR indicates a grid created with triangular elements that used automatic mesh refinement.

Table 5: Errors in energy balance for all cases with fuel segregations and non-bonds at different grid refinements.

Grid	Finer	Extra Fine
Domain	Base	
Fuel Segregation (FS)	0.000%	0.000%
Fuel + FS	0.046%	0.046%
Whole Model	0.000%	0.000%
	TC	
Fuel Segregation (FS)	-0.055%	-0.030%
Fuel + FS	0.019%	0.010%
Whole Model	0.000%	0.000%
	TL	
Fuel Segregation (FS)	0.001%	0.000%
Fuel + FS	0.019%	0.010%
Whole Model	0.000%	0.000%

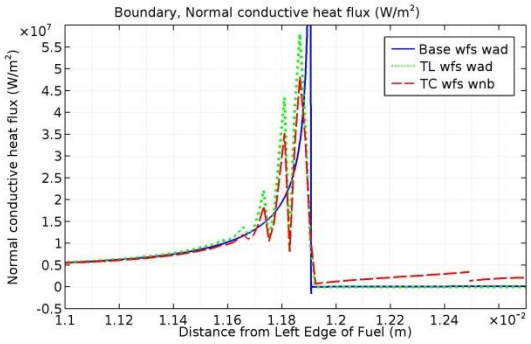

Figure 8 Oscillations experienced by TL and TC with the introduction of a simulated fuel segregation and non-bond along the modified boundary.

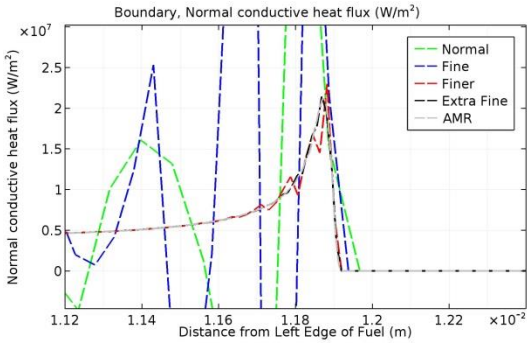

Figure 9 Oscillations near an adiabatic non-bond with TL for various grid refinements.

In addition to grid refinement, the effect of different element order on flux distortions was also examined. Figure 10 shows a TL model with coincident non-bond and fuel segregation with 3 different element orders compared to the base model with both defects using quadratic elements.

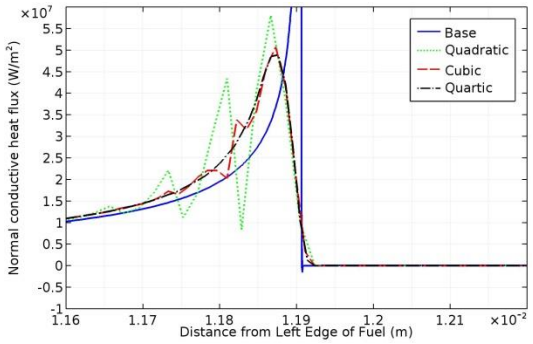

Figure 10 Oscillations near an adiabatic non-bond and fuel segregation with TL for various element orders.

6. Discussion

As modeled here, non-bonds create less severe hotspots than do fuel segregations. Coincident non-bonds and fuel segregations cause more severe hotspots as expected.

TC and TL both experience distortions in fluxes and temperatures relative to a traditional FEA model with a refined mesh.

Errors in energy balance are more severe with only a fuel segregation than in any other cases examined. The traditional FEA models only experienced errors in energy balance when modeling a non-bond.

Refining the mesh on TC and TL, as well as increasing the element order reduce the distortions in flux. Little improvement in flux is gained by going from an extra fine mesh to using adaptive mesh refinement. However, an AMR may optimally place the fine mesh where it is most needed.

7. Conclusions

The thermal contact and thin layer boundary features in COMSOL are compared with a conventional FEA modeling approach. Differences in temperature, conductive heat fluxes, and energy balances are assessed for an array of cases. Oscillations are observed along the non-bond boundary in boundary heat flux for the thin layer and thermal contact models that are not physical.

Both thin layer and thermal contact modeling options are similar in performance, but the thermal contact model offers flexibility that make it the more appealing option for this assessment. First, the thermal contact model allows for the inclusion of structural mechanic effects on the conductivity across the non-bond. While including structural mechanics is outside the scope of this current effort, it should eventually be incorporated into the model. Similarly, the thermal contact model can be used to account for the heat transfer through accumulated fission gases in the non-bond. This aspect is also outside the scope of the current project, however, it will also need to be incorporated in the future. Finally, and most relevant right now, using the thermal contact model provides a direct estimate of the conductivity of the non-bond. If the thin layer were used, a value for the conductivity across the non-bond would still be needed.

Care must be exercised in mesh development to ensure flux spikes and oscillations within the TL and TC boundary layer features are at acceptable levels. Additionally, increasing the order of the elements helps to reduce the distortions near discontinuities or steep gradients. While the local distortions attributed to the TC and TL models are acceptable for the thermal analysis, they may need to be revisited when thermal stress assessments are included in the plate fuel simulations.

9. References

1. Hilvety, N., & Chapman, T. G., HFIR Fuel Element Steady State Heat Transfer Analysis (No. ORNL-TM--1903). (1967)
2. Kirkpatrick, J. R.. Calculations for HFIR Fuel Plate Non-Bonding and Fuel Segregation Uncertainty Factors, (1990)
3. McLain, H. A., HFIR Fuel Element Steady State Heat Transfer Analysis, Revised Version (No. ORNL-TM--1904), (1967)
4. Giles Jr, G. E., Local analysis technique for the advanced neutron source reactor fuel defect studies. *Nuclear technology*, ***117*****(3)**, 306-315, (1997)